MODELING OF UNINTENDED HYDROGEN RELEASES FROM A FUEL CELL TRAM

Liu, B.[1], Pei, C.X.[1], Huang, T.[2], Zhao, M.B.[2], Ba, Q.X.[2], He, Q.[2], Li, M.[1], Christopher, D.M.[3], Li, X.F.[2,*]

[1]Technology Research Center, CRRC TANGSHAN CO., LTD., Tangshan 064000, China

[2]Institute of Thermal Science and Technology, Shandong University, Jinan 250061, China

[3]Key Laboratory of Thermal Science and Power Engineering of Ministry of Education, Tsinghua University, Beijing 100084, China

*** Corresponding author: lixf@email.sdu.edu.cn**

ABSTRACT

Hydrogen is a promising alternative energy carrier that has been increasingly used in industry, especially the transportation sector, to fuel vehicles through fuel cells. Hydrogen fuel cell vehicles usually have high pressure on-board storage tanks which take up large spaces to provide comparable ranges as current fossil fuel vehicles because of the low volumetric energy density of hydrogen. Therefore, hydrogen is also appropriate for large, heavy-duty vehicles that have more space than passenger vehicles. However, unintended hydrogen releases from a high-pressure vessel may result in serious consequences. Thus, hydrogen safety problems should be thoroughly studied to facilitate the promotion and commercialization of hydrogen energy. The CRRC Corporation Limited (CRRC) plans to use hydrogen to fuel urban rail transit systems to reduce the demand for urban power supplies. The present work modeled hydrogen releases and dispersion from on-board storage tanks of a fuel cell tram for three different release directions, that is, upward, lateral and forward, for both stationary and moving scenarios. The results show that the upward leaks form flammable clouds over the tram roof. The lateral leaks result in flammable clouds spread to the side of the tram, posing risks to neighboring vehicles, people and buildings. The forward leaks result in flammable clouds accumulating on the tram roof, directly threatening the safety of the vehicle. Additionally, the volume of flammable clouds decreases with the increase of vehicle speed. This work provides guidance for selecting hydrogen storage tank placement and the structure design of fuel cell trams.

Keywords: Hydrogen safety, fuel cell tram, hydrogen releases and dispersion, moving tram

1 INTRODUCTION

As a promising energy carrier, hydrogen has the advantages of renewable, clean, and efficient when used as a fuel. Hydrogen can help tackle many environmental problems especially carbon emissions [1-3]. Hydrogen has been used in many industrial sectors for a long time, and demands for hydrogen in the transport sector are soaring in recent years [4-6]. Hydrogen fuel cells are used to power vehicles from passenger cars to industrial trucks. Fuel cell vehicles (FCVs) benefit from a short refilling time of only a few minutes and a long driving range, which makes them more suitable for heavy-duty transportations. The CRRC Corporation Limited (CRRC) plans to use hydrogen to fuel urban rail transit systems to reduce the demand for urban power supplies. The infrastructure cost can be significantly lowered since the hydrogen fuel cell trams are autonomous with no requirements for overhead wires and other auxiliary equipment.

Hydrogen has a very low volumetric energy density so it needs to be stored onboard at very high pressures up to 70 MPa to provide enough driving range. Unintended hydrogen releases from a high pressure source will cause serious consequences since hydrogen is highly flammable [7-8]. Many studies have analyzed the hydrogen accumulation in an FCV to evaluate the risks of explosion and asphyxiation for different accident scenarios [9-10]. Hydrogen releases from vehicles will form flammable gas mixtures which may be ignited. Researchers have studied hydrogen releases and explosions for various scenarios like tunnels [11-14], large underground garages [15, 16], and residential garages [17]. Middha et al. [11] modeled the flammable gas mixture distributions in a tunnel and calculated the overpressures for the worst-case ignitions. Houf et al. [12] carried out a combined experimental and CFD modeling study to characterize hydrogen releases from a fuel-cell vehicle inside a tunnel, in which the full-scale CFD modeling was validated by a scaled model experiment. Kožuh [13] developed an approach to prevent hydrogen explosion in road tunnels by covering the ceiling with "hydrogen traps", which is a bunch of tubes having a diameter lesser than 1/3 of the detonation cell size. Li et al. [14] modeled hydrogen releases, dispersion and detonation in a tunnel using the all-speed CFD code GASFLOW-MPI. The temporal evolutions of the hydrogen concentration as well as the flammable regions were predicted numerically in the underground parking garage [15] and family four-car garage [17]. Zhao et al. [16] developed a hydrogen leak localization system based on measured concentration data in a scaled underground garage using two machine learning algorithms. Many studies focus on how to disperse the leaking hydrogen effectively using blowers and provides useful guidance to the first-responders [18, 19].

Previous studies mainly focus on hydrogen releases from stationary sources. However, accidental releases can also occur on a moving vehicle, which may pose unique risks to the vehicle or the surroundings. In this paper, hydrogen releases from a CRRC fuel cell tram were modeled to investigate the effects of release direction, tram speed, and leak flow rate on the flammable gas mixture distributions.

2 NUMERICAL MODELS

2.1 Geometry and Mesh

The model geometry is shown in Fig. 1, which was built based on a real-size tram. Hydrogen storage tanks and fuel cell modules were placed on the roof of the tram to make sure hydrogen will not directly flow into the tram in an accidental release. The hydrogen tanks were installed inside a metal frame so the whole set of the tanks has been simplified into a box. Most small elements on the roof were ignored to further simplify the geometry. The aerodynamic locomotive was well modeled to better simulate the real airflow as the tram moving.

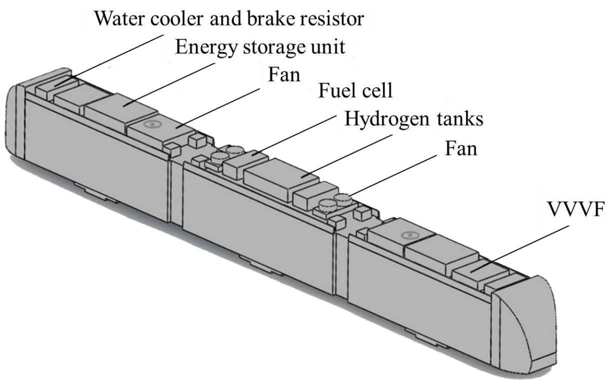

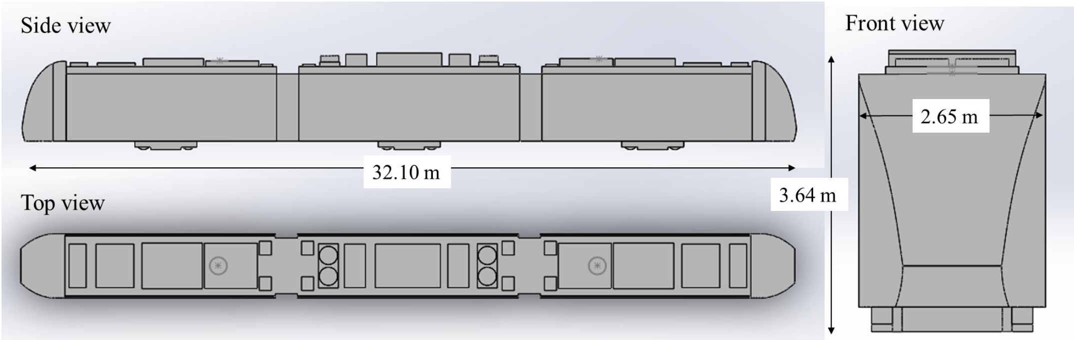

Fig. 1 Tram geometry.

The space was assumed to be symmetric since the leak and all the boundary conditions were symmetric. The total computational region was a quarter of a cylinder of radius 60 m and length 400 m, large enough that the boundaries have little effect on the flow around the vehicle. The tram front end was 100 m from the air inlet of the computational region to leave enough space for airflow and hydrogen dispersion in the back of the tram. Since the computational region is very large, two sets of meshes were combined to reduce the total element number. The space around the tram was discretized using tetrahedral elements while the outside space was meshed with hexahedrons, as shown in Fig. 2 (a). The "density box" and overset mesh technique was used to overlap a refined hexahedral mesh onto the tetrahedral mesh around the orifice since the flow velocity at the orifice was very high as shown in Fig. 2 (b).

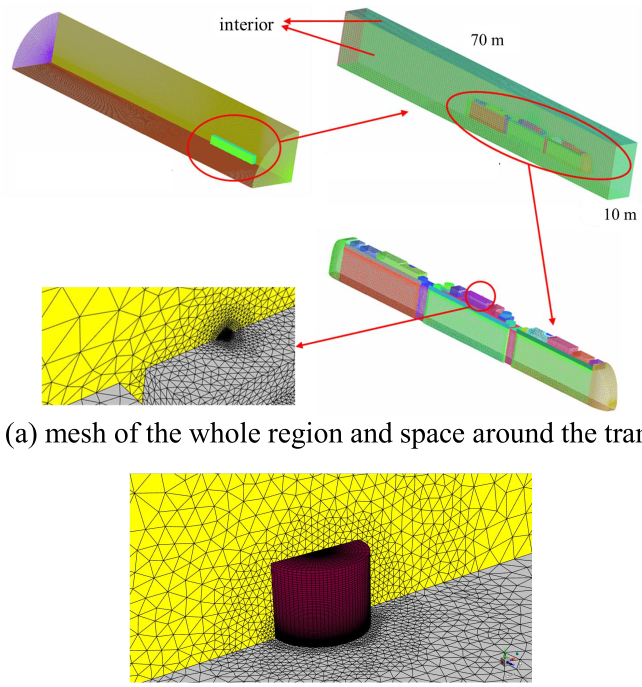

(a) mesh of the whole region and space around the tram

(b) mesh around the orifice

Fig. 2 Computational domain and mesh.

The pressure inside the hydrogen tank was 70 MPa, so highly underexpanded jets would form outside the leak orifice and made the modeling very computationally expensive. Therefore, a notional nozzle model [20] was used to calculate an effective leak radius to simplify the modeling. The leak nozzle diameter was 3 mm. The 100% leak is the worst case pipe rupture and the 10% leak is one case of pipe ruptures. The calculated effective radius was 25.4 mm for a 100% leak size and 8.03 mm for a 10%

leak size.

2.2 Modeling Approach

The hydrogen releases were modeled by solving the three-dimensional, steady state Navier-Stokes equations with the k-epsilon turbulence model and the species transport equation:

$$\nabla \cdot (\rho \vec{v} Y) = \nabla \cdot \left(\rho D + \frac{\mu_t}{Sc_t} \right) \nabla Y \tag{1}$$

where D is the diffusion coefficient, μ_t is the turbulent viscosity, Sc_t is the turbulent Schmidt number and Y is the hydrogen mass fraction. The advection terms were discretized with the second-order upwind scheme. The SIMPLE algorithm was used for pressure-velocity coupling. Fluent 19 was used for the simulations. The Fluent mass-flow-inlet type was chosen for the hydrogen inlet boundary condition. All the tram surfaces were set as wall boundary conditions. The downstream outlet boundary condition was set as a pressure-outlet. The surrounding air outlet boundary was set as a pressure outlet for stationary scenarios and as a moving wall for moving scenarios. The air-hydrogen mixture was modeled as an incompressible ideal gas with the gravitational constant set to 9.8 m/s^2.

The Molkov notional nozzle model [20] was used to simplify the modeling. Expansion of the Abel–Noble gas from the reservoir to the nozzle exit is isentropic, without losses in the flow in the Molkov notional nozzle model. There is no air entrainment to an expanding jet between the nozzle exit and the notional nozzle exit. The pressure at the notional nozzle exit is assumed to the atmospheric pressure and the speed at the notional nozzle exit is assumed to local sound speed. The boundary conditions (BCs) for stationary and moving scenarios are summarized in Table 1.

Table 1. Boundary conditions (BCs).

Surface	**BCs (stationary tram)**	**BCs (moving tram)**
Front surface of air region	Pressure inlet	Velocity inlet (-8.33 m/s, -19.44 m/s)
Lateral surface of air region	Pressure outlet	Moving wall (-8.33 m/s, -19.44 m/s)
Ground	Stationary wall	Moving wall (-8.33 m/s, -19.44 m/s)
Back surface of air region	Pressure outlet	
Tram surfaces	Stationary wall	
Hydrogen inlet	Mass flow rate inlet (0.239 kg/s for 100% leak size, 0.0239 kg/s for 10% leak size)	

There are two approaches available for modeling the moving tram in Fluent 19: the one, by making the tram stationary and letting air flows from the opposite direction; the other, by using the sliding mesh methodology. A comparison of using the two approaches is shown in Fig. 3. The calculated hydrogen distributions show that the results are almost the same. Hence, the airflow method was used in the present study since the sliding mesh method requires much more computational grids.

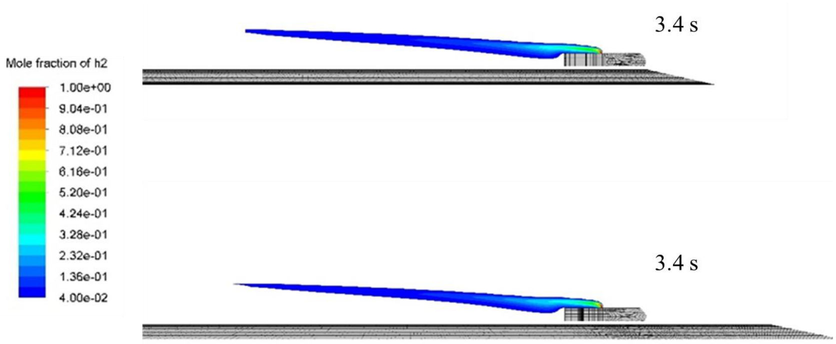

Fig. 3 Comparison of two modeling approaches (above: sliding mesh, below: airflow).

2.3 Grid Independence

Seven meshes with 2 to 3.7 million elements were used for grid independence checking. The calculated flammable gas volumes for upward releases with 100% leak size are shown in Fig. 4. The results were similar for meshes that had more than 2.45 million elements, so the results presented here are for the mesh with 2.7 million elements.

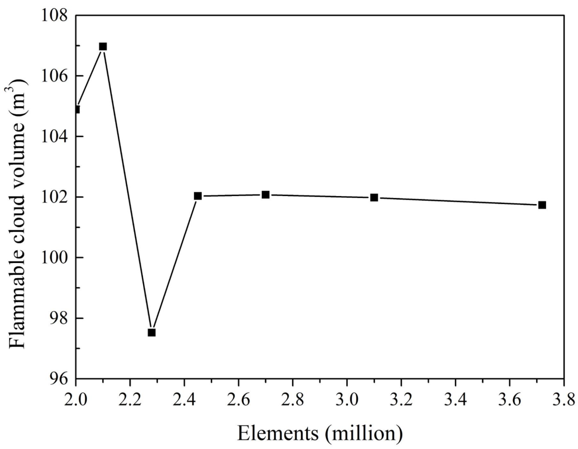

Fig. 4 Calculated flammable gas mixture volume using seven meshes.

3 RESULTS AND DISCUSSION

3.1 Upward Releases

The calculated flammable clouds of 100% upward releases with various tram speeds are shown in Fig. 5. Hydrogen flowed away from the tram for all three cases of stationary, 30 km/h and 70 km/h, so there was no direct safety concern posed for the tram if the hydrogen was not ignited. When the tram was stationary, the hydrogen jet was dominated by the initial momentum and accelerated by buoyancy force, which formed a large flammable cloud with a height of 21.85 m and a volume of 102.08 m^3. When the tram moved at a speed of 30 km/h, the hydrogen jet bent backward because of the air blowing and formed a flammable cloud with a maximum length of 14.35 m and a height of 5.60 m. The flammable cloud volume was 39.35 m^3, which is significantly smaller than that of a stationary case. When the tram moved at a speed of 70 km/h, the hydrogen jet bent more backward because of the stronger air blowing and formed a longer flammable cloud compared to the 30 km/h case. The flammable cloud was 18.08 m long and 3.64 m high and the volume was 24.22 m^3, which was the smallest among the three cases.

The predicted flammable clouds of 10% upward releases with various tram speeds are shown in Fig. 6. Smaller flammable clouds were formed compared to the 100% cases since the hydrogen mass flow rate was prominently smaller than the 10% case. The calculated flammable cloud volumes were 3.44 m^3 for the stationary case, 0.98 m^3 for the 30 km/h case, and 0.52 m^3 for the 70 km/h case.

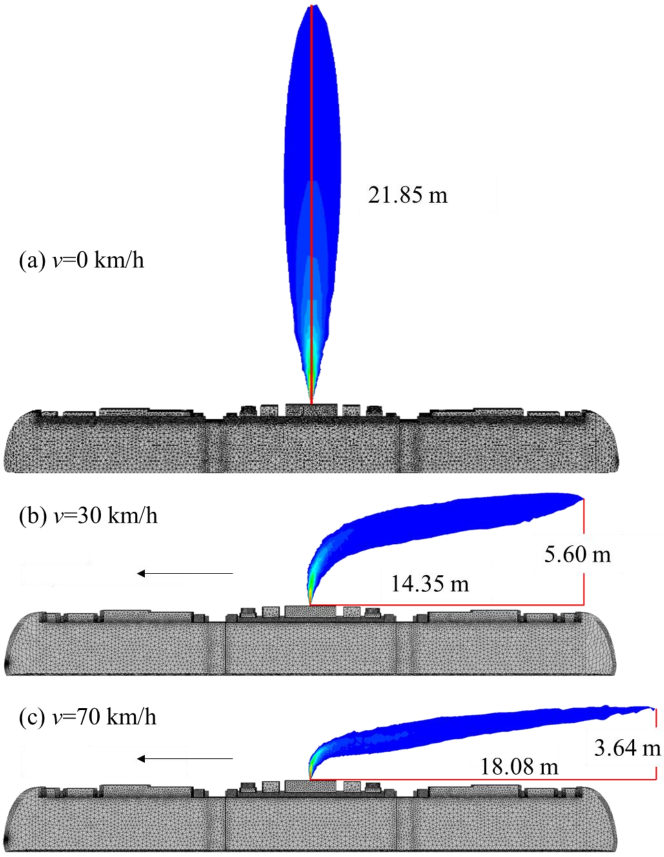

Fig. 5 Flammable clouds of 100% upward releases.

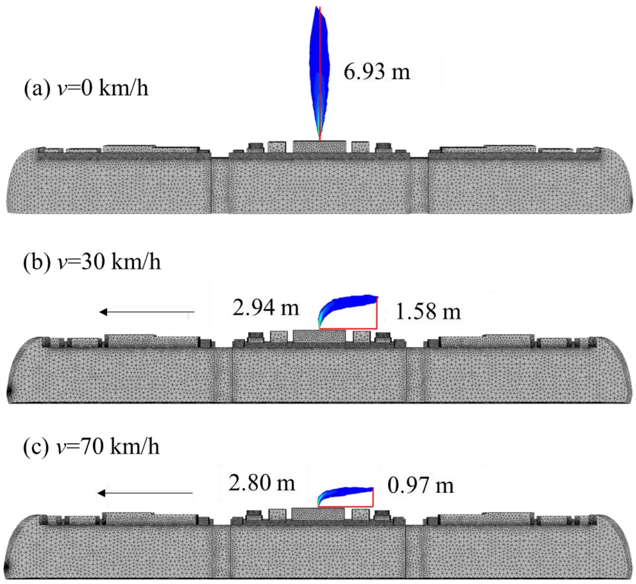

Fig. 6 Flammable clouds of 10% upward releases.

A 10% leak (or smaller) is more likely to happen compared to the 100% leak since the 100% leak requires a complete break of the pipe. The 100% leak represents the worst case that would happen in a serious crash. All cases had a flammable gas mixture flowing away from the tram which did not directly threaten the tram. However, an explosion could still damage the components on the roof if the gas mixture was ignited, especially when the tram was moving and the bent hydrogen jets were very close to the roof.

3.2 Lateral Releases

When the tram was not moving, a 100% horizontal, lateral release formed a flammable cloud that slightly rose because of the buoyancy effect in the far-field, as shown in Fig. 7. The flammable cloud had a volume of 119.50 m^3. The flammable cloud expanded horizontally to a maximum length of 23.39 m, which would pose great risks to neighboring vehicles, buildings, or people. When the tram was moving, the hydrogen jets bent because of the airflow from the opposite direction. The flammable clouds had a volume of 47.29 m^3 for the 30 km/h case and 23.02 m^3 for the 70 km/h case. A higher tram speed resulted in a smaller flammable cloud as expected.

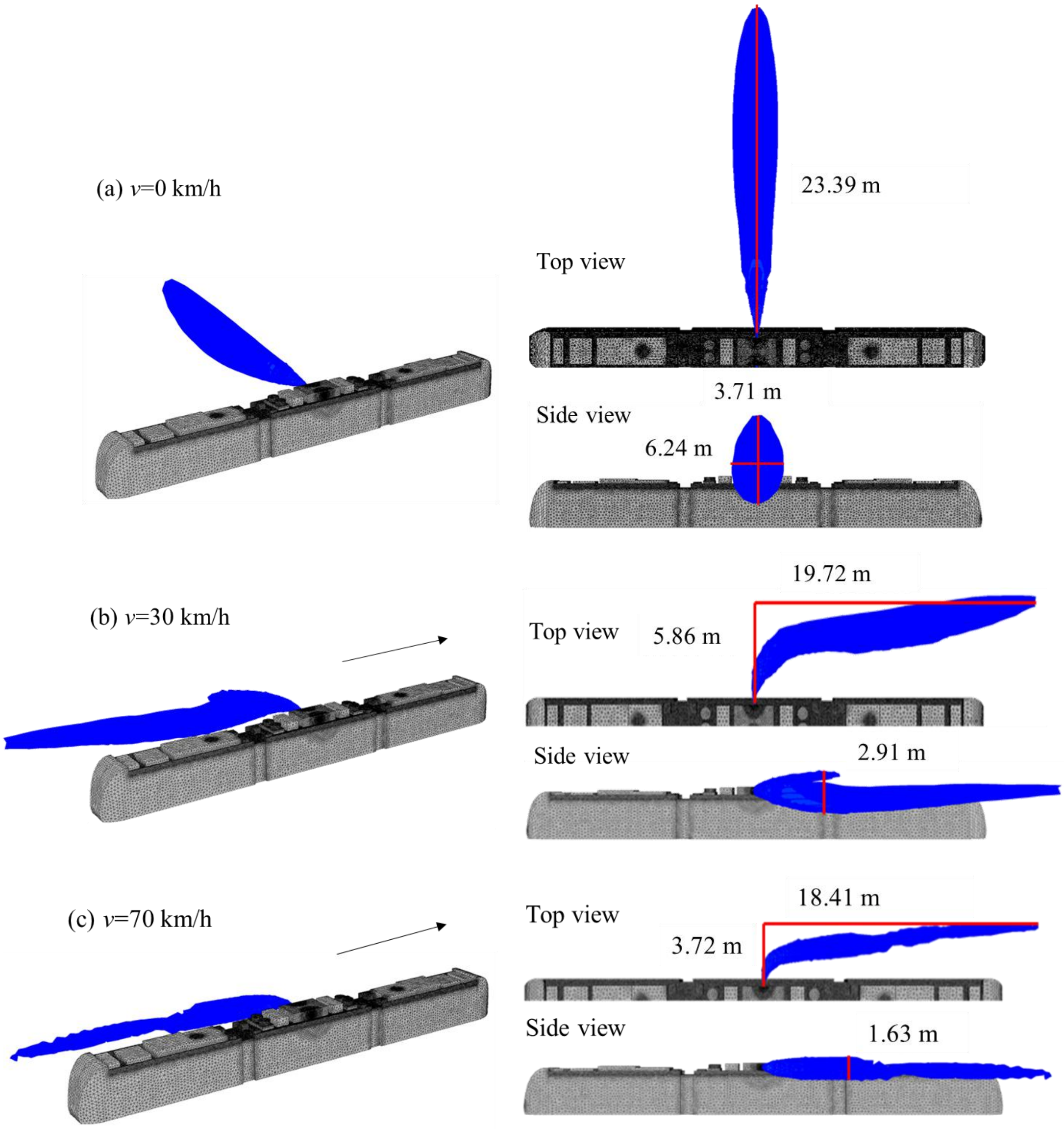

Fig. 7 Flammable clouds of 100% lateral releases.

The calculated flammable clouds of 10% lateral releases for various tram speeds are shown in Fig. 8. The 10% lateral releases also pose significant risks to the side of the leak. The calculated flammable cloud volume was 4.95 m^3 for the stationary case, 1.11 m^3 for the 30 km/h case, and 0.69 m^3 for the 70 km/h case.

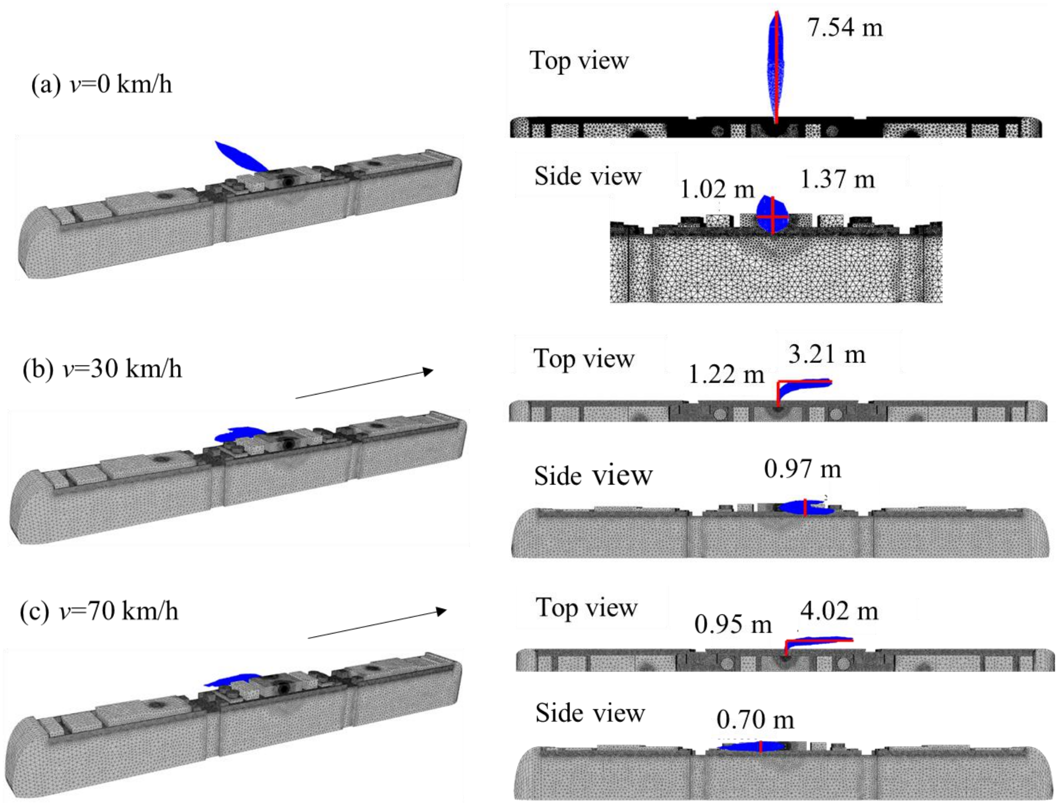

Fig. 8 Flammable clouds of 10% lateral releases.

3.3 Forward Releases

The calculated flammable clouds of 100% forward releases for various tram speeds are shown in Fig. 9. The released hydrogen accumulated on the roof because that there were many components on the roof with gaps between the roof and the components. The hydrogen jet impinged on the surface of the fuel cell unit and then moved backward and expanded to the whole roof of the second compartment when the tram was not moving. A large flammable gas mixture of 249.40 m^3 was formed because that the components obstructed the hydrogen dispersion. When the tram was moving, the hydrogen jets bent backward and accumulated on the roofs of the second and third compartments. The flammable clouds had a volume of 132.38 m^3 for the 30 km/h case and 54.43 m^3 for the 70 km/h case. Since the components on the roof mostly had electric wires connected to them, there was a high potential of ignition which would cause serious consequences.

The calculated flammable clouds of 10% forward releases for various tram speeds are shown in Fig. 10. The predicted flammable cloud volumes were 16.81 m^3 for the stationary case, 8.79 m^3 for the 30 km/h case, and 2.74 m^3 for the 70 km/h case, which were prominently smaller than those of 100% releases because of the smaller flow rates. However, the flammable gas mixture still accumulated on the roof of the second compartment, which would pose considerable risks to the tram.

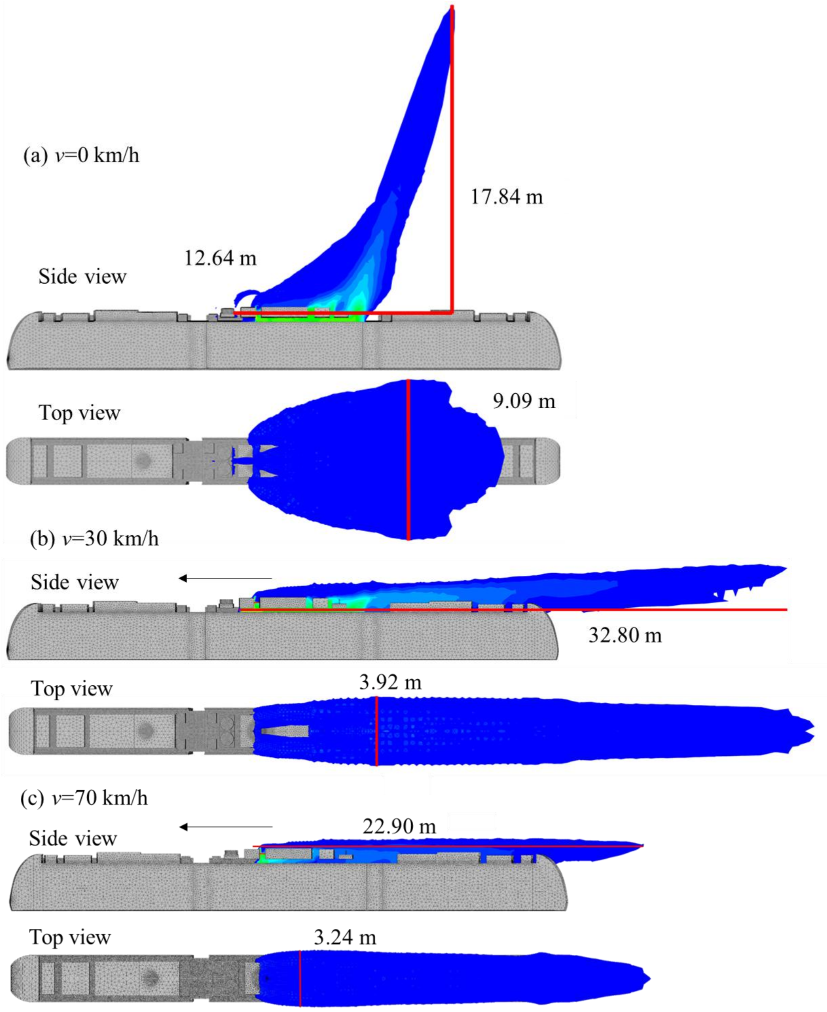

Fig. 9 Flammable clouds of 100% forward releases.

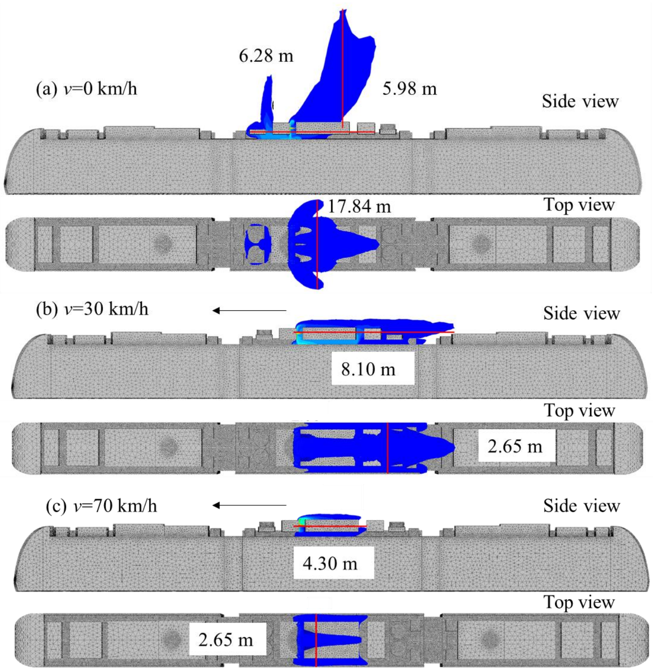

Fig. 10 Flammable clouds of 10% forward releases.

3.4 Comparison

The predicted flammable cloud volumes of different scenarios are compared in Fig. 11 for both 100% and 10% releases. The forward releases resulted in the largest flammable cloud for all cases because of the hydrogen accumulation on the roof and the air blowing against the jets. When the tram was not moving, the lateral releases formed larger flammable clouds than the upward releases, since the buoyancy force was in the same direction as the upward hydrogen jets and facilitated the hydrogen dispersion. When the tram was moving at a high speed (70 km/h), the air blowing was very strong and essentially facilitated the hydrogen dispersion, so the flammable clouds were almost the same size for the 100% releases. The flammable clouds were almost the same for the 10% releases for both 30 km/h and 70 km/h cases since the hydrogen flow rates were relatively small. However, the flammable cloud of 10% forward release was still visibly higher than those of upward and lateral releases, since the obstruction effects of the components on the roof should not be overlooked for the releases with a small flow rate.

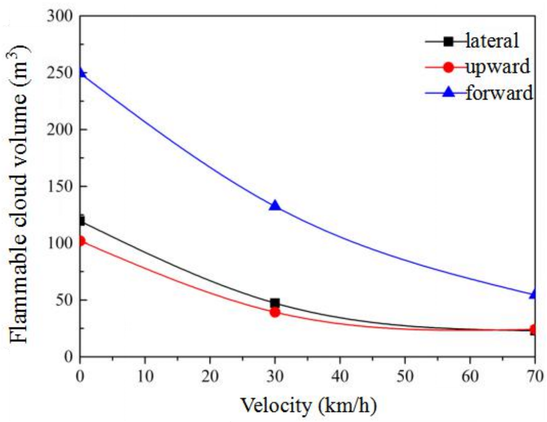

(a) 100% release

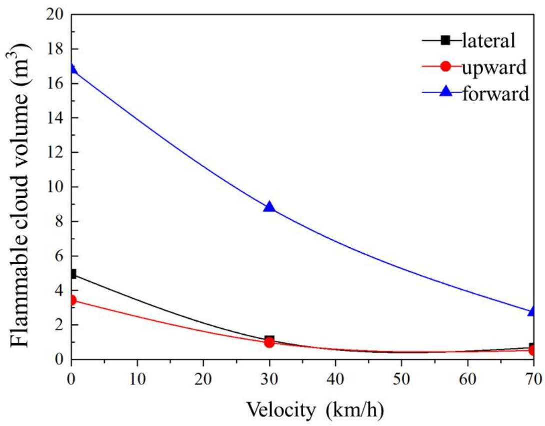

(b) 10% release

Fig. 11 Flammable cloud volumes

4 CONCLUSIONS

Unignited hydrogen releases and dispersion from on-board storage tanks of a CRRC fuel cell tram were modeled for both stationary of moving (30 and 70 km/h) scenarios. Three different release directions were studied, that is, upward, lateral, and forward. Though the upward releases did not directly threaten the tram, there were safety concerns once the released hydrogen was ignited since the bent hydrogen jets were very close to the roof when the tram was moving. The lateral releases pose great risks to the side of the leak because the hydrogen jets spread almost horizontally. The forward releases resulted in the largest flammable clouds and hydrogen accumulation on the roof because the components on the roof obstructed the hydrogen dispersion and the air blew against the hydrogen jets. The forward release formed a considerable flammable gas mixture on the roof even for a 10% leak and a high moving speed of 70 km/h because of the obstruction of components of the roof, which should not be overlooked since there were many electric wires having the potential to ignite the flammable gas mixture. The present results provide a useful reference for safety designs of the hydrogen fuel cell trams.

ACKNOWLEDGMENT

The National Natural Science Foundation of China (No. 51706125).

REFERENCES

1. Barbir F. Transition to renewable energy systems with hydrogen as an energy carrier. *Energy*, **34**, No. 3, 2009, pp. 308-312.
2. Panwar N L, Kaushik S C, Kothari S. Role of renewable energy sources in environmental protection: A review. *Renewable and Sustainable Energy Reviews*, **15**, No. 3, 2011, pp. 1513-1524.
3. Apak S, Atay E, Tuncer G. Renewable hydrogen energy and energy efficiency in Turkey in the 21st century. *International Journal of Hydrogen Energy*, **42**, No. 4, 2017, pp. 2446-2452.
4. Veziroglu A, Macario R. Fuel cell vehicles: State of the art with economic and environmental concerns. *International Journal of Hydrogen Energy*, **36**, No. 1, 2011, pp. 25-43.
5. Neef H J. International overview of hydrogen and fuel cell research. *Energy*, **34**, No. 3, 2009, pp. 327-333.
6. Zubaryeva A, Thiel C. Analyzing potential lead markets for hydrogen fuel cell vehicles in Europe: Expert views and spatial perspective. *International Journal of Hydrogen Energy*, **38**, No. 36, 2013, pp. 15878-15886.
7. Vladimir M. Fundamentals of Hydrogen Safety Engineering II. E Book at Bookboon.com, 2012.
8. Barilo N F, Weiner S C, James C W. Overview of the DOE hydrogen safety, codes and standards program part 2: Hydrogen and fuel cells: Emphasizing safety to enable commercialization. *International Journal of Hydrogen Energy*, **42**, No. 11, 2017, pp.7625-7632.
9. Salva J A, Tapia E, Iranzo A, et al. Safety study of a hydrogen leak in a fuel cell vehicle using computational fluid dynamics. *International Journal of Hydrogen Energy*, **37**, No. 6, 2012, pp. 5299-5306.
10. Yu X, Wang C, He Q. Numerical study of hydrogen dispersion in a fuel cell vehicle under the effect of ambient wind. *International Journal of Hydrogen Energy*, **44**, No. 40, 2019, pp. 22671-22680.
11. Middha P, Hansen O R. CFD simulation study to investigate the risk from hydrogen vehicles in tunnels. *International Journal of Hydrogen Energy*, **34**, No.14, 2009, pp. 5875-5886.
12. Houf W G, Evans G H, Merilo E, et al. Releases from hydrogen fuel-cell vehicles in tunnels. *International Journal of Hydrogen Energy*, **37**, No. 1, 2012, pp. 715-719.
13. Kožuh M. Preventing hydrogen detonations in road tunnels hydrogen trap concept. *International Journal of Hydrogen Energy*, **39**, No. 30, 2014, pp. 17434-17439.
14. Li Y, Xiao J, Zhang H, et al. Numerical analysis of hydrogen release, dispersion and combustion in a tunnel with fuel cell vehicles using all-speed CFD code GASFLOW-MPI. *International Journal of Hydrogen Energy*, **46**, No. 23, 2021, pp. 12474-12486.
15. Choi J, Hur N, Kang S, et al. A CFD simulation of hydrogen dispersion for the hydrogen leakage from a fuel cell vehicle in an underground parking garage. *International Journal of Hydrogen Energy*, **38**, No. 19, 2013, pp. 8084-8091.
16. Zhao M, Huang T, Liu C, et al. Leak localization using distributed sensors and machine learning for hydrogen releases from a fuel cell vehicle in a parking garage. *International Journal of Hydrogen Energy*, **46**, No. 1, 2021, pp. 1420-1433.
17. Li Y, Jiang J, Yu Y, et al. Numerical simulation of dispersion and distribution behaviors of

hydrogen leakage in the garage with a crossbeam. *SIMULATION: Transactions of the Society for Modeling and Simulation International*, **95**, No. 12, 2019, pp. 1229-1238.

18. Tamura Y, Takeuchi M, Sato K. Effectiveness of a blower in reducing the hazard of hydrogen leaking from a hydrogen-fueled vehicle. *International Journal of Hydrogen Energy*, **39**, No. 35, 2014, pp. 20339-20349.
19. Liu W, Christopher D M. Dispersion of hydrogen leaking from a hydrogen fuel cell vehicle. *International Journal of Hydrogen Energy*, **40**, No. 46, 2015, pp. 16673-16682.
20. Molkov V. Hydrogen safety engineering: The state-of-the-art and future progress[M]. Published by Elsevier Ltd, 2012.